Pharmaceutical Research, Vol. 23 No. 9, September 2006 (© 2006)
DOI: 10.1007/s11095-006-9044-z

Research Paper

Molecular Properties of Flurbiprofen and its Solid Dispersions with Eudragit RL100 Studied by High- and Low-Resolution Solid-State Nuclear Magnetic Resonance

Giulia Mollica,[1] Marco Geppi,[1,3] Rosario Pignatello,[2] and Carlo A. Veracini[1]

Received December 8, 2005; accepted April 25, 2006; published online August 9, 2006

Purpose. Investigation of the conformational and molecular dynamic properties of the acidic and sodium salt forms of Flurbiprofen and their solid dispersions with Eudragit® RL100, obtained by two different preparation methods (physical mixtures and coevaporates), and of the mixing degree between the two components in the dispersions.
Materials and Methods. ^{1}H and ^{13}C high-resolution solid state NMR techniques, including Single Pulse Excitation-MAS, CP-MAS, FSLG-HETCOR; low-resolution ^{1}H FID analysis; ^{1}H spin-lattice relaxation time measurements.
Results. Conformational, molecular packing and dynamic differences were observed between the two pure forms of flurbiprofen, as well as between the pure drugs and the corresponding coevaporates. In the coevaporates of the two flurbiprofen forms, drug and polymer appear intimately mixed; their chemical interactions were detected and characterized.
Conclusions. A combined analysis of several ^{13}C and ^{1}H high- and low-resolution solid state NMR experiments allowed the investigation of the conformational and dynamic properties of the pure drugs and of the solid dispersions with the polymer, as well as of the degree of mixing between drug and polymer and of the chemical nature of their interaction. Such information could be compared to the *in vitro* drug release profiles given by these solid dispersions.

KEY WORDS: coevaporates; conformational properties; cross-polarization magic-angle Spinning (CPMAS); drug-polymer interactions; FSLG-HETCOR; proton spin diffusion, spin-lattice relaxation times and FID analysis; ^{1}H and ^{13}C chemical shifts.

INTRODUCTION

Solid state NMR has revealed a particularly useful technique for the characterization of active pharmaceutical ingredients present in many solid pharmaceutical products, since it can be applied directly to the same physical state as their dispensed form. Most of the studies reported in this field concern drug polymorphism, that can usually be investigated from the analysis of standard ^{13}C CPMAS spectra, since ^{13}C chemical shifts are very sensitive to the different chemical environment experienced by the nuclei in different polymorphs (1–4). However, the possibility offered by solid state NMR of looking at different nuclear properties and/or nuclei, as well as the many sophisticated pulse sequences available nowadays (5), allow the application of this technique to obtain detailed information, such as molecular dynamics and conformational properties of both drug and carrier, and drug-carrier physical and chemical interactions, that can be eventually related to the bioavailability of the drug (6,7). In this respect, several mono- and bi-dimensional ^{1}H and ^{13}C high-resolution Solid-State NMR techniques have been recently combined by us to study the acidic and sodium salt forms of ibuprofen, and their solid dispersions with Eudragit RL100, obtained either as physical mixtures or coevaporates (7). The aspects investigated concerned the structural and dynamic properties of the two drug forms, as well as drug-polymer physical mixing and molecular interactions; the NMR information were related to the *in vitro* drug release profiles observed for the solid dispersions.

In the present paper we report an extension of the previous study to similar solid dispersions, where flurbiprofen is present in place of ibuprofen. Flurbiprofen [2-fluoro-α-methyl-[1,1′-biphenyl]-4-acetic acid; FLU, Fig. 1] is a non-steroidal anti-inflammatory drug (NSAID), extensively used for clinical treatment of rheumatoid arthritis, osteoarthritis, moderate pain and inflammatory diseases, particularly at the ophthalmic level (8–10). Recently attention has been focused on this as well as other NSAIDs for prevention and treatment of Alzheimer disease, given the ability displayed by FLU to reduce the production and secretion of β-amylase (11). Eudragit® Retard polymers are commonly used in the pharmaceutical technology in the coating of solid dosage forms and have been recently proposed for the preparation of

[1] Dipartimento di Chimica e Chimica Industriale, Università di Pisa, v. Risorgimento 35, 56126, Pisa, Italy.
[2] Dipartimento di Scienze Farmaceutiche, Università degli Studi di Catania, viale A. Doria 6, 95125, Catania, Italy.
[3] To whom correspondence should be addressed. (e-mail: mg@dcci.unipi.it)

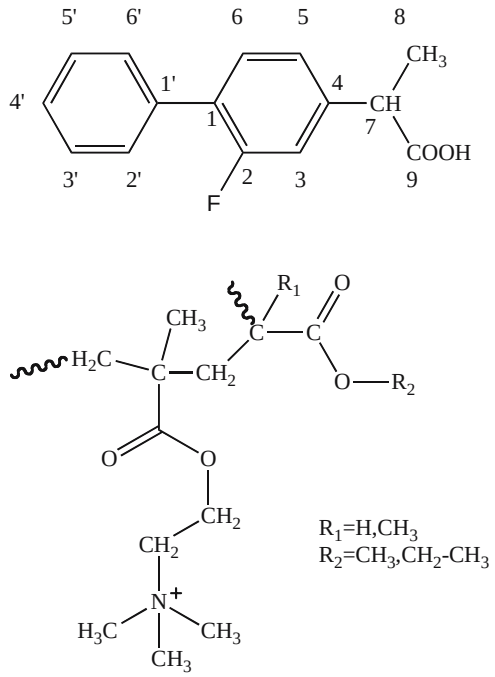

Fig. 1. Chemical structures of FLU-A (*top*) and RL (*bottom*).

controlled release systems, such as micro- and nanoparticles (12–14). In the present study, Eudragit RL100 matrix (RL) was used; this acrylic polymer has been specifically developed for pH-independent, delayed release from oral dosage forms. It is a water-insoluble, slightly swellable material based on neutral methacrylic acid esters with a small proportion of trimethylammonioethyl methacrylate chloride (Fig. 1). In particular, in RL the molar ratio of the quaternary ammonium groups to the neutral ester groups is 1:20 (corresponding to about 50 meq/100 g), making this polymer highly permeable to water. The acidic (FLU-A) and salt (FLU-S) forms of FLU were first characterized in order to highlight possible structural, conformational and dynamic differences. Then, their solid dispersions with RL were investigated, looking in particular at the differences induced on the molecular properties of the drug by the presence of the polymer, and at the degree of mixing and chemical interactions taking place in physical mixtures and coevaporates. In addition to the techniques already employed in the previous study on ibuprofen (7), in this case we also made use of time-domain low-resolution NMR techniques, such as on-resonance ^{1}H FID analysis, with the aim of further investigating, especially by comparative analyses, the dynamic behaviour of the systems studied.

The results obtained from solid state NMR have been compared with the *in vitro* drug release pattern from RL coevaporates loaded with FLU-A or FLU-S, to confirm how the interactions possibly occurring between the drug and polymer can affect the overall physico-chemical behaviour of these delivery systems.

MATERIALS AND METHODS

Samples

Flurbiprofen sodium salt (FLU-S) was purchased by Sigma-Aldrich Chimica s.r.l. (Milan-Italy) and was used as received. The corresponding acidic form (FLU-A) was prepared by treating an aqueous solution of FLU-S with diluted acetic acid. The white precipitate was filtered, washed with water and recrystallized from ethanol. The structure of FLU-A was confirmed by spectroscopical analysis and m.p. determination. Eudragit RL100 (RL) was kindly gifted by Rofarma Italia srl (Gaggiano, Italy). The polymer was used as received in order to prepare two different kinds of solid dispersion with the drug, coevaporates and physical mixtures, according to a published procedure (13). Briefly, the physical mixtures were prepared by simply triturating drug and polymer (1:2 by weight) in a mortar without solvent; coevaporates were obtained by co-dissolving drug and polymer (1:2 by weight) in absolute ethanol at room temperature, stirring the mixture for 4–6 h and then removing the solvent under high vacuum in a rotary evaporator at a maximum external temperature of 40°C. The samples were stored in closed amber glass vials at room temperature. The 1:2 drug-to-polymer ratio was selected in these experiments among different ratios previously tested for NSAIDs/Eudragit Retard solid systems (15). This choice represents a good balance between the two needs of having a good drug solubility in the polymer matrix, and a sufficient sensitivity for both drug and polymer components in the spectroscopic analysis.

In Vitro Dissolution Tests

The drug release from the polymeric matrix was evaluated at room temperature for 24 h. Fifty-milligram samples of the coevaporate or physical mixture or an equivalent amount of pure drugs (about 17 mg) were dispersed in 100 ml of water and stirred at 100 rpm. At predetermined time intervals one-ml aliquots of the solution were withdrawn and replaced with the same volume of water. The samples were filtered (0.45 μm PTFE membrane filters) and the amount of dissolved drug was measured by UV spectrophotometry at 247 nm (Shimadzu UV-1601). The drug release was calculated as the percent dissolved drug with respect to the initial drug loading (33.3/100 mg of coevaporates or physical mixtures).

NMR Methods

All the high resolution NMR experiments were performed on a Varian InfinityPlus 400 double channel spectrometer operating at the ^{1}H Larmor frequency of 399.89 MHz and the ^{13}C frequency of 100.56 MHz, equipped with two CP-MAS probes for rotors with an outer diameter of 3.2 and 7.5 mm. Both the ^{13}C and ^{1}H 90° pulses were 4.2 and 1.9 μs for the 7.5 and 3.2 probes, respectively.

The CP-MAS spectra have been recorded using constant rf power for both channels or a linear ramp (16) for the ^{13}C channel power during the contact time. Continuous wave decoupling was used for all samples except for FLU-A and FLU-S, for which a SPINAL-64 (17) decoupling scheme was employed. The CP-MAS spectra were recorded with a contact time of 1–2 ms and spinning frequencies of 5–7.5 kHz. The HETCOR experiments on FLU-A and FLU-S were both performed with 240 scans, 146 rows, and a contact time of 0.2 ms, while the spinning rate was 6.5 kHz for FLU-

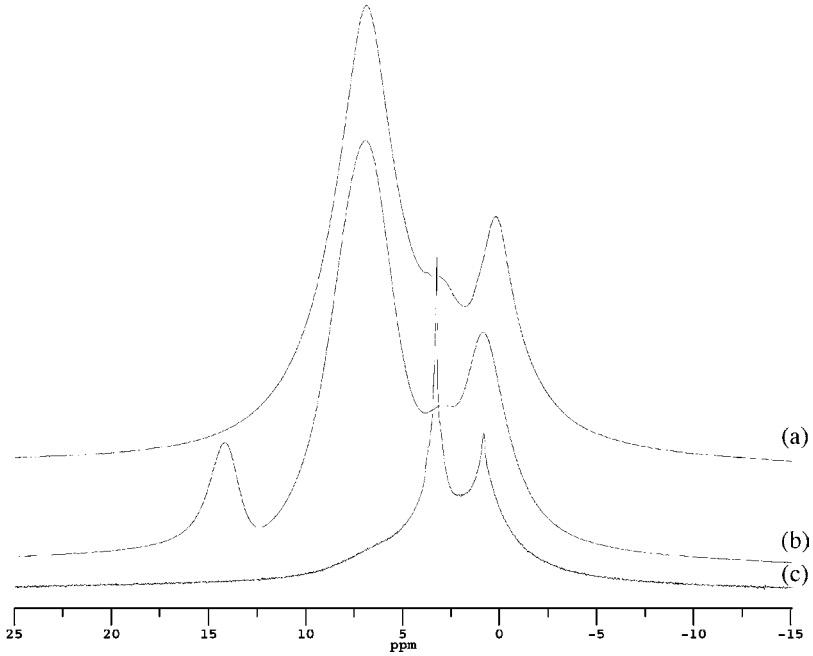

Fig. 2. ^{1}H-MAS spectra of: (a) FLU-S, (b) FLU-A, and (c) RL. All the spectra were acquired at a spinning speed of 25 kHz.

A and 7.5 kHz for FLU-S. ^{1}H T_1 relaxation times measurements were performed through the ^{13}C-detected Inversion Recovery Cross Polarization technique (18). ^{1}H MAS experiments were recorded at a spinning frequency of 25 kHz.

Both the on resonance FID analysis and the ^{1}H T_1 measurements in low resolution conditions were performed on a single channel Varian XL 100 spectrometer interfaced with a Stelar DS-NMR acquisition system: in this case the ^{1}H 90° pulse length was 2.8 μs. ^{1}H FIDs were recorded by means of the Solid Echo technique (19), using an echo delay of 12 μs and a dwell time of 1 μs. The pulse sequence Inversion Recovery with attached solid echo was used for measuring ^{1}H T_1. All the measurements have been performed at 25.0 ± 0.2°C.

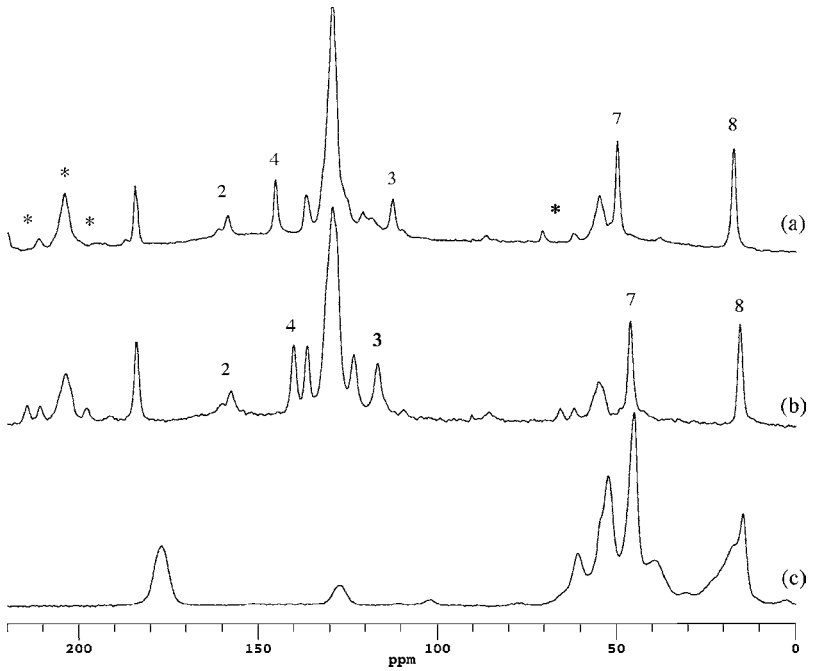

Fig. 3. ^{13}C CP-MAS spectra of: (a) FLU-S, (b) FLU-A, and (c) RL. The spinning speed was 7.5 kHz for FLU-A and FLU-S and 5 kHz for RL. The labelling of the peaks refers to Fig. 1. *Asterisks* denote spinning sidebands.

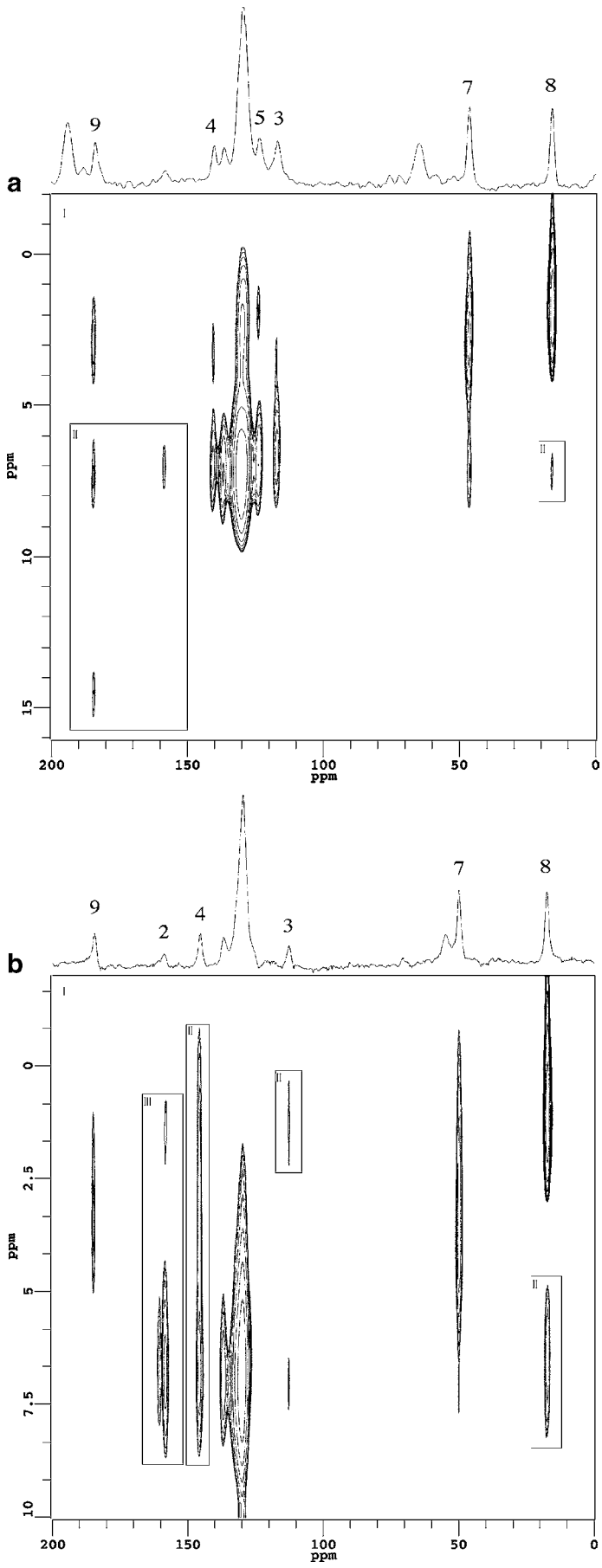
a
9
4
5
3
7
8
ppm
200
150
100
50
0
b
9
2
4
3
7
8
ppm
200
150
100
50
0

RESULTS AND DISCUSSION

Pure Components

^1H Spectra

Expansions of the ^1H MAS spectra of FLU-A and FLU-S, recorded at a spinning frequency of 25 kHz, are shown in Fig. 2, together with the corresponding spectrum of RL.

The assignment of the peaks is quite straightforward: for FLU-A (Fig. 2b) four different signals are clearly distinguishable, corresponding to methyl (≈1 ppm), methine (≈3 ppm), aromatic (≈7 ppm) and acidic (≈14 ppm) protons. Unfortunately the residual line width does not allow a better spectral resolution and therefore the different aromatic signals cannot be distinguished.

In the spectrum of FLU-S (Fig. 2a) the same group of resonances has been observed, with the obvious exception of that due to the acidic protons. However, some noticeable differences are present in the chemical shift values between FLU-A and FLU-S, mainly concerning the peak of the methyl protons. This difference (about 0.7 ppm) is too large to be explained with the sole different chemical structure between the two forms of FLU, and therefore suggests the presence of significant differences in either conformational properties or molecular packing, that will be further discussed also on the basis of ^{13}C and ^1H–^{13}C HETCOR experiments.

The ^1H-MAS spectrum of RL (Fig. 2c) shows three heavily superimposed peaks and its interpretation has been discussed in (7): the signal at 1 ppm is due to all the aliphatic protons, with the exception of those close to the ester groups, that give rise to the large resonance centered at about 3.5 ppm; the narrow peak at the same chemical shift arises instead from the protons of the trimethylammonium groups, the minor line width being in agreement with the fast dynamic processes experienced by these groups.

^{13}C Spectra and ^1H–^{13}C HETCOR Maps

The ^{13}C CP-MAS spectra of the acidic and sodium salt forms of FLU, together with the corresponding spectrum of RL, are shown in Fig. 3, while in Fig. 4 the ^1H–^{13}C FSLG-HETCOR maps of FLU-A and FLU-S are reported.

The relatively small line widths (about 100–150 Hz) observed in the ^{13}C spectra of FLU-A indicate that it is crystalline, confirming the previously reported X-Ray diffraction (PXRD) data (13), while slightly larger line widths (150–250 Hz) are present in the spectra of FLU-S. This difference could be in principle ascribable to a higher static disorder present in FLU-S. However, other effects, as for instance differences in anisotropic bulk magnetic susceptibility, possibly due to different degrees of aromatic stacking, cannot be ruled out, and might themselves provide an explanation of the experimental behaviour (20,21).

The assignment of the ^{13}C spectrum of FLU-A (Fig. 3b) has been previously performed by Yates *et al.* (22), while for FLU-S (Fig. 3a) the interpretation of the spectrum has been carried out on the basis of the comparison between the ^{13}C CP-MAS spectra and the ^1H–^{13}C HETCOR maps of the two drug forms (Fig. 4). The resulting assignments are shown in Table I.

In particular, the peaks resonating at 145.2 and 112.9 ppm, exhibiting the largest shifts with respect to the spectrum of FLU-A, have been assigned to carbons 4 and 3, respectively, thanks to the FLU-S HETCOR map (Fig. 4b). This has been possible by observing the strong correlation between the carbons resonating at 145.2 ppm and methine protons, and a similar HETCOR correlation profile between the peak at 112.9 ppm and that ascribable to carbon 2 (158.6 and 161.3 ppm), easily recognizable because of the $^1J_{C–F}$ doublet.

As already pointed out in the description of ^1H MAS spectra, also the differences observed in the ^{13}C spectra and HETCOR maps of FLU-A and FLU-S must be discussed not only in terms of their different chemical structure, expected to mainly affect the chemical shifts of the signals of the carbonyl and nearest aliphatic carbons, but also taking into account possible different crystalline packing, conformational and dynamic behaviour, that can be particularly important in solid state spectra.

By comparing the ^{13}C chemical shifts of FLU-A and FLU-S, several differences can be outlined. Passing from FLU-A to FLU-S some shifts towards higher frequencies for aliphatic CH and CH_3 signals have been recorded, qualitatively expected by replacing the carboxyl moiety with the carboxylate one. However, these shifts are larger than those predicted by semi-empirical calculations for solution state spectra, based on the mere chemical structural changes (3.8 *vs* 2.7 and 1.8 *vs* 1.5 ppm for methine and methyl carbons, respectively). Nonetheless, the most significant differences are visible in the aromatic spectral region, that should be substantially unaffected by the different chemical structures. In particular, carbons 2 and 4 give rise to high-frequency shifts by about 1.0 and 5.0 ppm, respectively, while carbon 3 shifts towards lower frequencies by 4.0 ppm. These changes clearly indicate that FLU-A and FLU-S experience quite different conformational and/or crystal packing situations, as already hypothesized on the basis of ^1H spectra. This point could be further clarified by analyzing the 2D-HETCOR maps, showing dipolarly coupled proton–carbon pairs, mostly determined by their spatial proximity. In addition to the correlation expected on the basis of the chemical structure of FLU (for instance the methyl protons are obviously correlated to methyl, methine and carboxylic carbons), there are other correlations that shed light on the molecular conformational behaviour. In particular, by looking at methyl protons, in FLU-S they are correlated to aromatic carbons 3 and 2, indicating that the methyl group is closest to the side of the phenyl ring where the fluorine atom is present. A very different situation has

◀ **Fig. 4.** ^1H–^{13}C HETCOR maps of: (a) FLU-A, (b) FLU-S. The correlation peaks shown in the different regions, labeled by *roman numbers* in the map, were sampled at different threshold levels for the sake of clarity; the maximum peak intensities (in a.u.) are: 100 in I and 8 in II for FLU-A; 100 in I, 8 in II and 5 in III for FLU-S. The correlation peaks relative to ^{13}C spinning sidebands have been removed for simplifying the interpretation of the maps. Both the experiment were performed using 146 rows and a contact time of 0.2 ms, while the spinning speed was 6.5 kHz for FLU-A and 7.5 kHz for FLU-S. The labelling of the ^{13}C peaks refers to Fig. 1.

Table I. Assignment of ^{13}C Solid-State Spectra for FLU-A and FLU-S

	^{13}C Chemical shifts (ppm)	
Nucleus	FLU-A	FLU-S
1′	136.4	136.2
2[a]	157.7	158.6
	160.2	161.3
3	116.9	112.9
4	140.2	145.2
5	123.5	–
7	46.4	50.2
8	16.0	17.8
9	183.9	184.4
1, 6, 2′, 3′, 4′, 5′, 6′	128.5	129.1

The labelling of the nuclei refers to Fig. 1.
[a] The doublet observed for this carbon is due to the $^{1}J_{C-F}$ scalar coupling (26).

been observed in FLU-A, where the same protons are correlated to the aromatic carbon 5, therefore revealing that here the methyl group lies on the opposite part of the phenyl ring, in agreement with the observed aromatic ring shifts.

For a discussion of the ^{13}C spectrum of pure RL, shown in Fig. 3c, details can be found in a previous study (7).

Solid Dispersions

^{1}H *Spectra*

The ^{1}H MAS spectra of both the physical mixtures and coevaporates of the two forms of FLU with RL are shown in Fig. 5.

The spectra of both the physical mixtures (Fig. 5b and d) substantially coincide with the weighted superposition of the spectra of the individual components (Fig. 2), suggesting that no noteworthy interactions between drug and polymer occur.

On the contrary, the spectra of the two coevaporates (Fig. 5a and c) exhibit some interesting differences. The ^{1}H spectrum of the FLU-A coevaporate clearly shows the disappearance of the acidic proton signal, occurring at about 14.0 ppm in the spectrum of the corresponding physical mixture, already observed for the ibuprofen-RL coevaporate (7). This clearly indicates that the dimeric structures present in pure FLU-A, formed by two FLU-A molecules by means of hydrogen bonds involving the acidic groups, are destroyed in the coevaporate.

For both FLU-A and FLU-S coevaporates, the signals of the trimethylammonium group of the polymer undergo significant modifications with respect to the spectra of the pure components and physical mixtures, experiencing a broadening (more evident in the case of FLU-A) and a strong shift towards higher frequencies (by about 2.0 and 0.6 ppm for FLU-A and FLU-S, respectively), in complete agreement with what previously observed for the corresponding coevaporates of ibuprofen (7). This seems to indicate a change of both chemical environment and dynamics of the trimethylammonium groups: the shift of the resonance frequency is compatible with an interaction of this group with the FLU-A carboxyl and FLU-S carboxylate moieties, and the broadening suggests that the reorientational motions of these groups significantly slow down in the coevaporate with respect to the pure, amorphous polymer, as it is expected in presence of strong interactions with the drug.

As far as the aromatic signals are concerned, the line narrowing observed in the coevaporates with respect to physical mixtures, more evident in the case of FLU-A, is in agreement with the breaking of the drug crystalline structure,

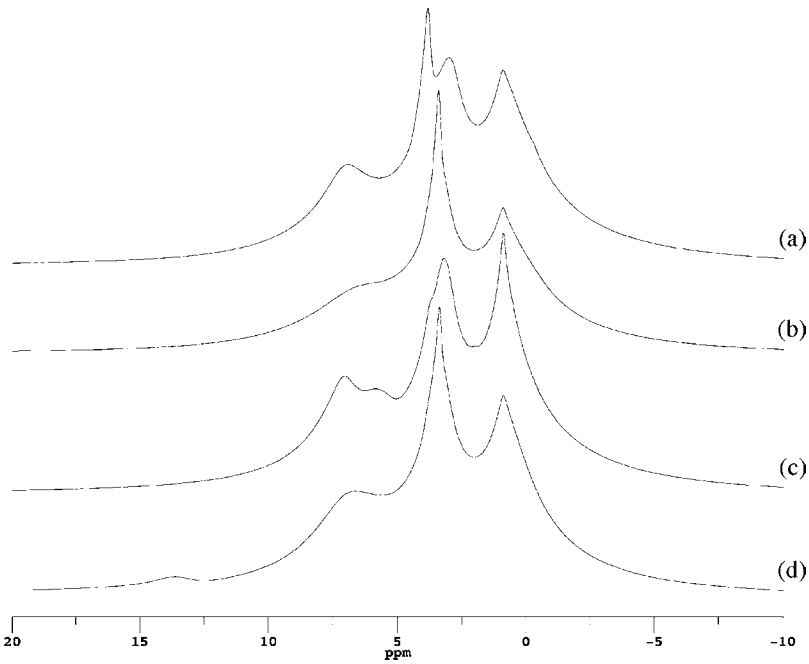

Fig. 5. ^{1}H-MAS spectra of: (a) FLU-S/RL coevaporate, (b) FLU-S/RL physical mixture, (c) FLU-A/RL coevaporate, (d) FLU-A/RL physical mixture. All the spectra were acquired at a spinning speed of 25 kHz.

resulting in either a faster dynamics, already observed for the corresponding coevaporate formed by the acidic form of ibuprofen (7), or in a reduction of the linebroadening due to anisotropic bulk magnetic susceptibility (20).

^{13}C *Spectra*

The ^{13}C CP-MAS spectra of the solid dispersions of FLU-A and FLU-S with RL are shown in Fig. 6. Due to the low drug-to-polymer ratio (1:2 w/w), the spectra of the solid dispersions are dominated, in their aliphatic and carbonyl regions, by the signals of RL carbons. However, the aromatic region contains signals of drug carbons only, being free from RL resonances, with the exception of a spinning side-band of the carbonyl signal at about 117 ppm, thus rendering possible the observation of spectral changes induced by the possible drug-polymer interactions.

As previously observed for ^{1}H spectra, the ^{13}C spectra of the physical mixtures of FLU-A (Fig. 6d) and FLU-S (Fig. 6b) with RL are simply the weighted superposition of the spectra of the pure components. This confirms that no significant modifications in both drug and carrier molecular properties occur following their mixing, and therefore that no detectable interactions between the two components take place. In particular, on passing from pure components to physical mixtures, no changes have been observed for the signals ascribed to the aromatic carbon 4 (resonating at 140.2 and 145.2 ppm in the spectra of pure FLU-A and FLU-S, respectively), that revealed to be very sensitive to conformational or molecular packing properties of the drug, as previously discussed.

In contrast to the physical mixtures, and in agreement with what observed for ^{1}H spectra, the ^{13}C spectra of the two coevaporates (Fig. 6a and c) show some noticeable differences with respect to the spectra of the individual components and of the physical mixtures, mainly concerning frequency shifts of some peaks and a significant linebroadening. The shifts are particularly evident for carbons 4 (quaternary aromatic) and 9 (carboxylic) in FLU-A. The former gives a high-frequency shift by 3.8 ppm (from 140.2 to 144.0 ppm) on passing from pure FLU-A to the corresponding coevaporate. On the basis of the discussion previously reported in explaining the chemical shift differences between the two pure forms of FLU, this indicates that strong conformational and/or molecular packing changes occur in FLU-A when the coevaporate is formed. On the other hand, the peak relative to the carboxyl moiety (resonating at 183.9 ppm in pure FLU-A) seems to be no longer present in the spectrum of the coevaporate. This is possibly due either to a dramatic linebroadening, already observed for the corresponding coevaporate of ibuprofen (7), or to the occurrence of drug-polymer interactions. However, the hypothesis that an esterification of FLU-A during the preparation of the coevaporate could take place cannot be completely ruled out at this stage, and further investigations to this regard are currently in progress. Other spectral changes are observed in the region of methyl resonances, even though less evident because of the presence of the asymmetric, broad and intense peak arising from the methyl groups of RL. A close inspection reveals that in the spectra of the two coevaporates the peaks relative to the drug methyl carbons shift towards higher frequencies with respect to the spectra of the pure drugs and physical mixtures.

As far as the line width differences are concerned, these mainly affect the resonances of the drug carbons, that appear quite broader in the spectra of both the coevaporates. This is particularly evident for aromatic (for both FLU-A and FLU-S) and FLU-S carboxylate signals, experiencing minor super-

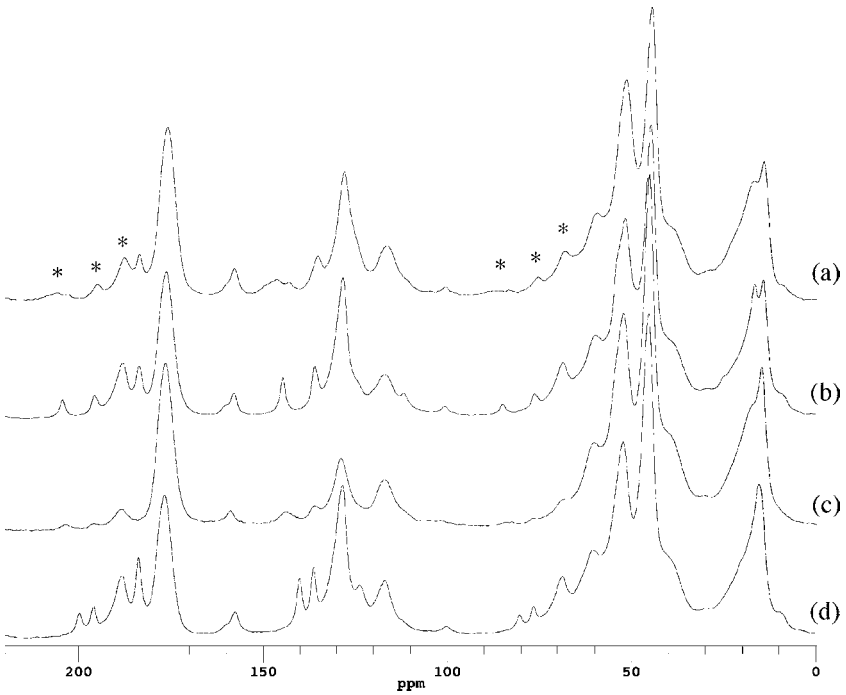

Fig. 6. ^{13}C CP-MAS spectra of: (a) FLU-S/RL coevaporate, (b) FLU-S/RL physical mixture, (c) FLU-A/RL coevaporate, (d) FLU-A/RL physical mixture, recorded with a spinning speed of 6 kHz. *Asterisks* denote spinning sidebands.

positions with polymer signals. Since anisotropic bulk magnetic susceptibility should rather give rise to line narrowing, as already pointed out for ^{1}H spectra, the linebroadening observed in coevaporates is ascribable either to a larger distribution of isotropic chemical shifts, arising in turns from a distribution of chemical environments for the same carbons belonging to different drug molecules, or to a considerable alteration of the molecular dynamics of the drugs caused by the mixing with the polymer. In any case, this is a clear indication of a strong drug-polymer interaction occurring in coevaporates. However, if the linebroadening had a dynamic nature, on one side the motional process affecting the line width should be ascribable to the whole molecule, since all the signals of the drugs give rise to linebroadening; on the other side, the linebroadening should be due to some interference of a typical motional frequency with an instrumental frequency, such as the magic angle spinning or decoupling ones (23). Since experiments performed at different spinning and/or decoupling frequencies do not show any detectable change in the line widths, this hypothesis can be safely ruled out. Therefore the linebroadening should be explained in terms of a wider distribution of chemical environments, that is expected given the amorphous nature of the coevaporates (13) because of either a distribution of conformational situations or a more disordered molecular packing. The linebroadening is particularly large for carbon 4 in both FLU-A and FLU-S coevaporates, suggesting that this carbon experiences a very broad distribution of conformational situations; in the case of the FLU-S coevaporate a doublet-like structure is present (Fig. 6a), suggesting the presence of two preferred conformers. Given the noticeable sensitivity of the chemical shift of this resonance to the conformational properties of the aliphatic chain, previously discussed, we can conclude that a particularly wide distribution of conformations is present for the aliphatic chains of both FLU-A and FLU-S in their corresponding coevaporates.

^{1}H FID Analysis

This analysis consists in recording the on-resonance decay of the time domain NMR signal and fitting it to a linear combination of different analytical functions. This may allow, in simple systems, quantitative information about the presence and the number of motionally distinct regions of a sample to be obtained: each function corresponds to one of the motionally distinguishable domains of the sample and its best-fitting parameters (such as, for instance, the spin-spin relaxation time T_2) can be directly related to the dynamic properties of that domain, while the weight of each function within the linear combination is proportional to the number of protons in that domain. In complex systems, like those here investigated, the interpretation of different decay functions in terms of physically distinguishable regions of the sample can result problematic.

The results of the FID analysis for both the pure samples and the four solid dispersions are shown in Table II.

All the experimental FIDs were fitted to a linear combination of analytical functions chosen among Gaussian, exponential, Pake, Weibullian and Abragamian. After an accurate screening of all the possible combinations, the functions really employed in our case were the first three.

Exponential ($E(t)$) and Gaussian ($G(t)$) functions, whose expressions are shown below, are characterised by their transversal relaxation time T_2, in general higher T_2 values meaning higher mobility:

$$E(t) = e^{-\frac{t}{T_2}}$$

$$G(t) = e^{-\left(\frac{t}{T_2}\right)^2}$$

The Pake ($P(t)$) function is derived as the inverse Fourier transform of the original expression in the frequency domain (24), and has the following expression:

$$P(t) = \sqrt{\frac{\pi}{6}} \cdot e^{\left(-\frac{1}{2}\beta^2 t^2\right)} \cdot \left(\frac{\cos \alpha t}{\sqrt{\alpha t}} C\left[\sqrt{\frac{6\alpha t}{\pi}}\right] + \frac{\sin \alpha t}{\sqrt{\alpha t}} S\left[\sqrt{\frac{6\alpha t}{\pi}}\right] \right)$$

Where

$$\alpha = \frac{3\gamma^2}{4R_{HH}^3}$$

With γ the proton gyromagnetic ratio, and R_{HH} the distance between two nearest dipolarly coupled protons: in complex coupled systems, in which it is not possible to identify isolated spin couples, R_{HH} must be thought as an average value. β can be seen as inversely proportional to the T_2 of the "Gaussian" component of the Pake function, which refers to the not nearest dipolarly coupled protons. C and S are the approximated Fresnell functions. The exponential and Gaussian T_2, β and R_{HH}, together with the weight of each function, were varied in the fitting.

Both the FIDs of FLU-A and FLU-S could be well reproduced by a linear combination of a Pake (P) and an Exponential function (E1). In Fig. 7 the fitting of the FLU-S FID is reported as an example. The weights of the two functions are very similar in the two samples, in agreement with their little different chemical structure, and in all the cases their best-fitting parameters are typical of very rigid phases. The larger R_{HH} value obtained for FLU-S is in agreement with the less effective crystal packing with respect to FLU-A, due to the absence of dimeric structures formed by hydrogen bonds. The RL FID is well fitted by a linear combination of three functions, two Gaussians, indicated as G1 and G2, with T_2 values of ~12 and ~37 μs, respectively, characterizing two rigid domains with distinguishable dynamic behaviour, and an exponential with a $T_2 \sim 1.0$ ms (E2), corresponding to a very mobile phase. Because of the large structural heterogeneity of the polymer, the assignment of the different FID components to regions experiencing different dynamics in the sample is not straightforward. However, the very short T_2(G1) (within the rigid lattice limit) indicates that this function is ascribable to fractions of the polymer not experiencing motions with characteristic frequencies higher than tens kHz, reasonably mostly represented by the polymer main chains; G2, instead, exhibits a slightly longer T_2 value, and therefore must be associated to regions experiencing some restricted dynamics, such as, for instance, terminal main chains or hindered side-chains. On the contrary, the long T_2 value and the low percentage (5.5%) of E2 suggest that this function could be associated

Table II. FID Analysis Results for FLU-A, FLU-S, RL and the Corresponding Physical Mixtures (PM) and Coevaporates (*C*)

Fit function	Gaussian (G1)		Exponential (E2)		Gaussian (G2)		
Sample	wt.%	T_2 (μs)	wt.%	T_2 (μs)	wt.%		T_2 (μs)
RL	74.2	12.4	5.5	1,034	20.3		36.8
	Exponential (E1)				Pake(*P*)		
	wt.%	T_2 (μs)			wt.%	β (s^{-1})	R_{HH} (Å)
FLU-A	54.4	9.6			45.6	28,422	1.63
FLU-S	55.6	15.3			44.4	29,992	1.74
PM FLU-A	59.4	17.9	3.5	831	37.2	39,497	1.78
C FLU-A	61.9	18.0	2.3	301	35.7	52,633	1.80
PM FLU-S	59.6	16.9	4.3	1,020	36.1	43,962	1.74
C FLU-S	60.2	17.7	4.5	556	35.3	47,445	1.78

For each function weight percentage (wt.%) and decay parameters (T_2 for Gaussian and exponential functions, R_{HH} and β for the Pake function) are reported.

with most of the $[-N(CH_3)_3]^+$ groups, experiencing fast rotational motions.

The FIDs of all the four solid dispersions investigated could be well reproduced by using a linear combination of E1, E2 and *P*. Even though the detailed assignment of these functions, as well as a strict comparison with the FID results found for the pure components, cannot be performed, due to the complexity of the systems, some useful conclusions can be reliably drawn. First of all, it must be noticed that both E1 and *P* functions are characterized by very short relaxation

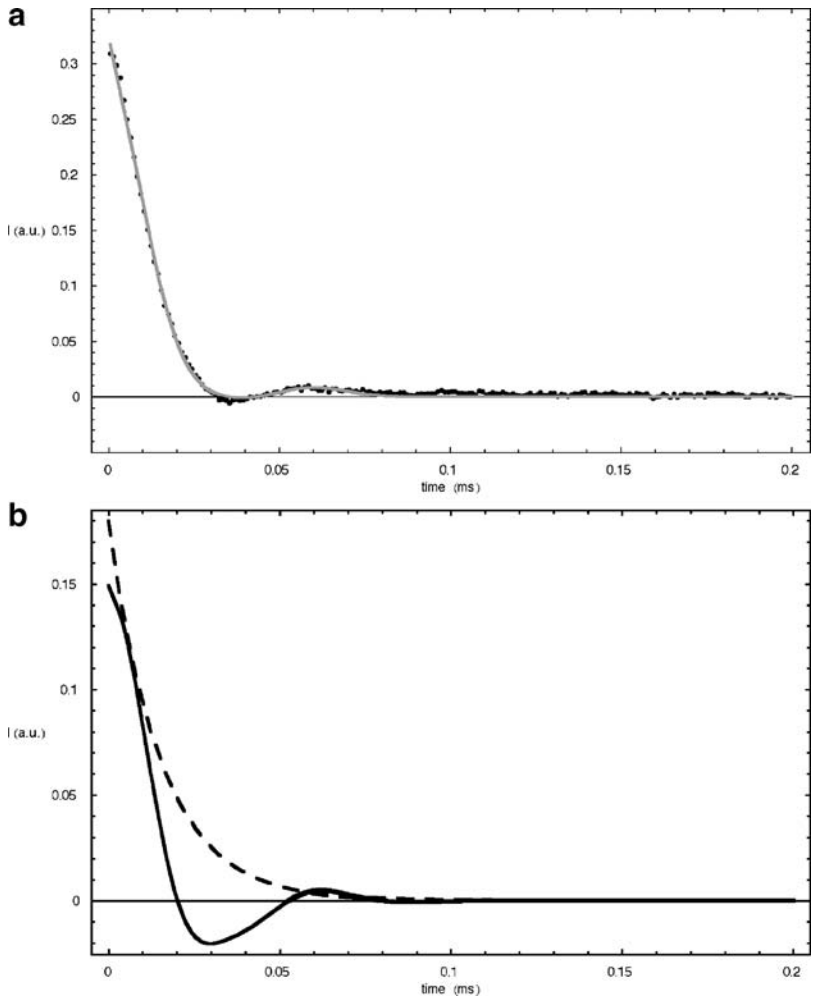

Fig. 7. ^{1}H FID analysis of FLU-S: (a) experimental and fitted FID, (b) contribution of individual fitting functions E1 (*dashed line*) and P (*full line*). The FID was recorded by a solid echo experiment, using an echo delay of 12 μs and a dwell time of 1 μs.

Table III. ^{1}H Spin-Lattice Relaxation Times (s) Measured for FLU-A, FLU-S, RL and the Corresponding Physical Mixtures (PM) and Coevaporates (*C*), Using Either Low- or High-Resolution Techniques, as Described in the Experimental Section

	25 MHz Low resolution			400 MHz High resolution	
FLU-A		2.22		2.7	
FLU-S		0.73		1.3	
RL		0.11		0.7	
				FLU	RL
PM FLU-A	2.05		0.11	2.0	0.8
wt.%	22		78		
C FLU-A		0.12		0.8	0.8
PM FLU-S	0.56		0.10	1.1	0.7
wt.%	27		73		
C FLU-S		0.13		0.8	0.8

For the high-resolution measurements on solid dispersions the average relaxation times measured for Flurbiprofen and RL components are reported. For the low-resolution measurements on the physical mixtures the two components of the FID decay are reported, each with its corresponding weight percentage (wt.%).

decays, and therefore must be associated to very rigid parts of the samples, while the function E2 corresponds to the most mobile fractions of the dispersions, and have been therefore mainly assigned to polymeric $[-N(CH_3)_3]^+$ groups. Due to its low weight percentage, the interpretation of the component E2 is somewhat open to doubt. However, the observation of a quite regular trend for T_2(E2) in passing from pure RL to physical mixtures and coevaporates strongly suggests that these data can be interpreted in terms of dynamics of trimethylammonium groups. Indeed, a T_2(E2) value is observed in physical mixtures which is very similar to that determined in pure RL, while it is 2–3 times shorter in coevaporates, thus indicating that the dynamics of trimethylammonium groups is not strongly affected by the presence of the drug in physical mixtures, while it is significantly slowed down in coevaporates, in agreement with the establishment of electrostatic interactions between the drug polar moieties and the polymeric trimethylammonium groups themselves.

^{1}H T_1 Analysis

The degree of mixing between the two components of the solid dispersions has been investigated through the measurement of proton spin-lattice relaxation times in the laboratory frame (T_1) under both high- and low-resolution experimental conditions. In fact, in solid samples the energy of the spin system is usually redistributed amongst the different protons via homonuclear dipolar couplings before being exchanged with the surrounding lattice. This process, known as spin diffusion, tends to average the relaxation times of the different protons in a sample to a single value. This average is complete in the case of a sample homogeneous on a 100 Å scale, while different relaxation times can be measured for protons belonging to different domains when these domains have average linear dimensions greater than 100 Å (25).

Given the scarce resolution of ^{1}H spectra achievable, even in fast MAS conditions, ^{1}H T_1 relaxation times were measured, exploiting the high resolution of the ^{13}C spectra, by means of the Inversion Recovery CP-MAS experiment. The results are shown in Table III. In the experiments performed on the pure component samples (FLU-A, FLU-S and RL) a single T_1 value was measured for all the protons, as expected. In both the physical mixtures two different average T_1 values could be revealed, one corresponding to the protons

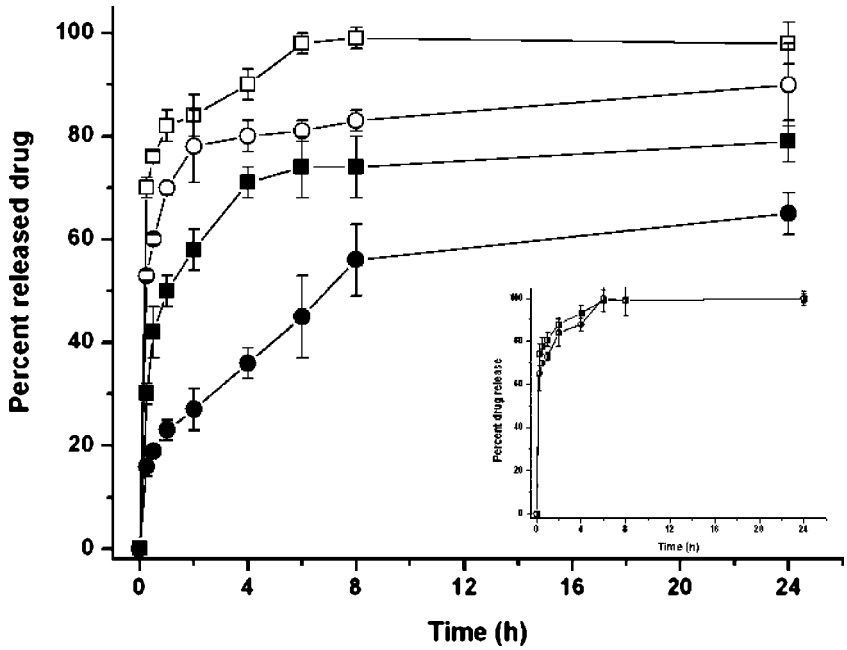

Fig. 8. *In vitro* dissolution patterns in water at room temperature of FLU from FLU-A/RL and FLU-S/RL coevaporates and physical mixtures. *Squares* refer to FLU-S, *circles* to FLU-A; *empty and filled* symbols refer to physical mixtures and coevaporates, respectively. The inset shows the dissolution profile of pure drugs.

of the drug and the other to those of the polymer, that represent partial averages of the relaxation times measured for the pure components. On the contrary, a single relaxation time was measured for all the protons in both the coevaporates. These results are validated by the ^1H T_1 measurements performed by Inversion-Recovery with direct ^1H observation, under low-resolution conditions (see Table III). Bi- and mono-exponential recoveries are observed for physical mixtures and coevaporates, respectively. Even though in this case the absence of spectral resolution does not allow to attribute the two relaxation components to specific protons in the sample, their weights are in excellent agreement with the number of protons in the drug and the polymeric phases.

These results clearly indicate that drug and polymer are not intimately (i.e., on a 100 Å scale) mixed in the physical mixtures, confirming the observation, performed by ^1H and ^{13}C spectra, that no significant interactions between drug and polymer occur in these samples. In the coevaporates, instead, drug and polymer domains have average dimensions smaller than 100 Å, the samples resulting homogeneous on that spatial scale, in agreement with the interactions previously detected between these two components from both ^1H and ^{13}C spectral analysis.

In Vitro Drug Release Assay

To gather comparative information with the NMR studies, coevaporates and physical mixtures FLU-A and FLU-S with RL were submitted to a dissolution test (13). As expected, the sodium salt of the drug displayed a quite rapid leakage from the coevaporate into the external medium (water) (Fig. 8), confirming the absence of strong interactions with RL. In fact, despite the drug was dispersed within the polymer network, its dissolution characteristics were prevalent. Conversely, FLU-A/RL coevaporates showed a typical modified-release pattern, with a gradual and prolonged leakage from the polymer microparticles.

Drug release from both the physical mixtures was higher (Fig. 8), confirming the absence of a significant association of the drug with RL when the components were simply mechanical mixed. When the drug was dispersed as its sodium salt, the release profile showed a very rapid leakage of the drug, with a burst release of about 76% of the dispersed drug within 15 min. These findings further suggest that the dissolution properties of the drug drove the overall release mechanism. The amount of drug released after 24 h using the FLU-S form were higher than that one measured with the FLU-A form, and reinforced our hypothesis of a synergistic physical and chemical interactions between this polymer network and acidic host molecules.

CONCLUSIONS

Following a similar study previously performed on ibuprofen-Eudragit RL100 solid dispersions (7), high-resolution ^1H and ^{13}C solid state NMR techniques have been used to investigate the structural, conformational and dynamic properties of two different forms (acid and sodium salt) of the NSAID flurbiprofen, in this case also supported by low-resolution proton FID analysis. The same techniques, together with the measurement of proton spin-lattice relaxation times in the laboratory frame (T_1), allowed us to get information also on the physical mixing and the chemical interactions between these drug forms and the Eudragit RL100 polymer in samples prepared by different methods (physical mixtures and coevaporates).

While the assignment of the solid state ^{13}C spectrum of FLU-A had already been performed in the literature (22), that of FLU-S has been interpreted here with the aid of the bidimensional FSLG-HETCOR technique. Remarkable conformational differences between FLU-A and FLU-S, concerning the relative position of the aliphatic chain with respect to the fluorinated aromatic ring, could be highlighted. No significant drug-polymer interactions could be revealed for the physical mixtures, while the coevaporates of both FLU-A and FLU-S resulted intimately mixed on a 100 Å spatial scale, as observed by ^1H T_1s; moreover, interactions involving the polymeric trimethylammonium group and the carboxyl/carboxylate function of the drug were observed by both ^1H and ^{13}C spectra. These interactions were also confirmed by the structural and dynamic modifications induced in the coevaporates with respect to the pure components and/or the corresponding physical mixtures, observed by the ^1H and ^{13}C MAS spectra, as well as the ^1H low-resolution FIDs. In the coevaporates, the drug molecules appear more disordered, since their crystalline structure is destroyed by the interaction with the amorphous polymer, also causing a stiffening of the polymer trimethylammonium groups. Such interactions result stronger in the FLU-A coevaporate with respect to the FLU-S one, in agreement with what previously observed for ibuprofen (7).

The *in vitro* drug release experiments supported the conclusion that no strong interaction occurred in the physical mixture between the drug, in both the acid and salt forms, and RL matrix. However, and according to the NMR evidences, when the drug-polymer mixture was obtained from a co-solution (coevaporates), a strong interaction occurred, in particular with the acid drug form; in this case, in fact, the release of FLU is slower and results from the contribution of both drug dissolution characteristics and its diffusion through the polymer network.

Similarly to our previous paper (7), this study further supports the usefulness of solid-state NMR studies in predicting the interactions that occur between a drug and a polymer, and their agreement with common experimental data, such as the drug release profile from the resulting polymeric delivery system.

REFERENCES

1. R. K. Harris. *Polymorphism and Related Phenomena*, in *Encyclopedia of NMR*, vol. 6:3734–3740. In D. M. Grant and R. K. Harris (eds.), Wiley, Chichester, 1996.
2. P. A. Tishmack, D. E. Bugay, and S. R. Byrn. Solid state nuclear magnetic resonance spectroscopy-pharmaceutical applications. *J. Pharm. Sci.* **92**:577–610 (2003).
3. S. R. Vippagunta, H. G. Brittain, and D. J. W. Grant. Crystalline solids. *Adv. Drug Deliv. Rev.* **48**:3–26 (2001).
4. D. E. Bugay. Characterization of the solid state: spectroscopic techniques. *Adv. Drug Deliv. Rev.* **48**:43–65 (2001).
5. S. P. Brown and H. W. Spiess. Advanced solid-state NMR methods for the elucidation of structure and dynamics of molecular, macromolecular, and supramolecular systems. *Chem. Rev.* **101**:4125–4155 (2001).

6. D. M. Schachter, J. Xiong, and G. C. Tirol. Solid state NMR perspective of drug-polymer solid solutions: a model system based on poly(ethylene oxide). *Int. J. Pharm.* **281**:89–101 (2004).
7. M. Geppi, S. Guccione, G. Mollica, R. Pignatello, and C. A. Veracini. Molecular properties of Ibuprofen and its solid dispersions with Eudragit RL100 studied by Solid-State Nuclear Magnetic Resonance. *Pharm. Res.* **22**:1544–1555 (2005).
8. W. R. Finch. Review of the dosing regimens for flurbiprofen. A potent analgesic/anti-inflammatory agent. *Am. J. Med.* **80**:16–18 (1986).
9. W. W. Buchanan and Y. B. Kassam. European experience with flurbiprofen. A new analgesic/anti-inflammatory agent. *Am. J. Med.* **80**:145–152 (1986).
10. R. Schalnus. Topical nonsteroidal anti-inflammatory therapy in ophthalmology. *Ophthalmologica* **217**:89–98 (2003).
11. L. Gasparini, E. Ongini, D. Wilcock, and D. Morgan. Activity of flurbiprofen and chemically related anti-inflammatory drugs in models of Alzheimer's disease. *Brain Res. Rev.* **48**:400–408 (2005).
12. R. Pignatello, M. Ferro, G. De Guidi, G. Salemi, M. A. Vandelli, S. Guccione, M. Geppi, C. Forte, and G. Puglisi. Preparation, characterisation and photosensitivity studies of solid dispersions of diflunisal and Eudragit RS100® and RL100®. *Int. J. Pharm.* **218**:27–42 (2001).
13. R. Pignatello, M. Ferro, and G. Puglisi. Preparation of solid dispersions of nonsteroidal anti-inflammatory drugs with acrylic polymers and studies on mechanisms of drug-polymer interaction. *AAPS PharmSciTech* **3**:art. 10 (2002).
14. R. Pignatello, C. Bucolo, G. Spedalieri, A. Maltese, and G. Puglisi. Flurbiprofen-loaded acrylate polymer nanosuspensions for ophthalmic application. *Biomaterials* **23**:3247–3255 (2002).
15. R. Pignatello, D. Spadaro, M. A. Vandelli, F. Forni, and G. Puglisi. Characterization of the mechanism of interaction in ibuprofen-Eudragit RL100 coevaporates. *Drug Dev. Ind. Pharm.* **30**:277–288 (2004).
16. G. Metz, X. L. Wu, and S. O. Smith. Ramped-amplitude Cross-Polarization in Magic-Angle-Spinning NMR. *J. Magn. Reson. A* **110**:219–227 (1994).
17. B. M. Fung, A. K. Khitrin, and K. Ermolaev. An improved broadband decoupling sequence for liquid crystals and solids. *J. Magn. Reson.* **142**:97–101 (2000).
18. R. Kitamaru, F. Horii, and K. Murayama. Phase structure of lamellar crystalline polyethylene by solid-state high-resolution ^{13}C NMR: detection of crystalline-amorphous interphase. *Macromolecules* **19**:636–643 (1986).
19. J. G. Powles and J. H. Strange. Zero time resolution nuclear magnetic resonance transients in solids. *Proc. Phys. Soc.* **82**:6–15 (1963).
20. D. L. VanderHart, W. L. Earl, and A. N. Garroway. Resolution in ^{13}C NMR of organic solids using high-power proton decoupling and magic-angle spinning. *J. Magn. Reson.* **44**: 361–401 (1981).
21. P. Hodgkinson. Heteronuclear decoupling in the NMR of solids. *Prog. Nucl. Magn. Reson. Spectrosc.* **46**:197–222 (2005).
22. J. R. Yates, S. E. Dobbins, C. J. Pickard, F. Mauri, P. Y. Ghi, and R. K. Harris. A combined first principles computational and solid-state NMR study of a molecular crystal: flurbiprofen. *Phys. Chem. Chem. Phys.* **7**:1402–1407 (2005).
23. W. P. Rothwell and J. S. Waugh. Transverse relaxation of dipolar coupled spin systems under rf irradiation: detecting motions in solids. *J. Chem. Phys.* **74**:2721–2732 (1981).
24. E. W. Hansen, P. E. Kristiansen, and B. Pedersen. Crystallinity of polyethylene derived from solid-state proton NMR free induction decay. *J. Phys. Chem. B* **102**:5444–5450 (1998).
25. L. Calucci, L. Galleschi, M. Geppi, and G. Mollica. Structure and dynamics of flour by solid state NMR: effects of hydration and wheat aging. *Biomacromolecules* **5**:1536–1544 (2004).
26. G. Antonioli and P. Hodgkinson. Resolution of C-13-F-19 interactions in the C-13 NMR of spinning solids and liquid crystals. *J. Magn. Reson.* **168**:124–131 (2004).